LAWRENCE
LIVERMORE
NATIONAL
LABORATORY

LLNL-TR-703909

Surrogate Measurements of Actinide (n,2n) Cross Sections with NeutronSTARS

R. J. Casperson, J. T. Burke, R. O. Hughes, O. A. Akindele, J. D. Koglin, B. Wang, A. Tamashiro

September 27, 2016

Disclaimer

This work performed under the auspices of the U.S. Department of Energy by Lawrence Livermore National Laboratory under Contract DE-AC52-07NA27344.

Surrogate Measurements of Actinide (n,2n) Cross Sections with NeutronSTARS

R. J. Casperson[1], J. T. Burke[1], R. O. Hughes[1], O. A. Akindele[2], J. D. Koglin[1], B. Wang[1], and A. Tamashiro[3]

1. Lawrence Livermore National Laboratory
2. University of California Berkeley
3. Oregon State University

Introduction

Directly measuring (n,2n) cross sections on short-lived actinides presents a number of experimental challenges: scattered beam can produce neutron backgrounds in the detectors, fission can produce a substantial neutron background, and created a target with a short-lived isotope can be extremely difficult. Direct techniques require on the order of grams of target material, which simply isn't possible for short-lived targets. The surrogate reaction technique is an experimental method for measuring cross sections on short-lived isotopes [1], and it provides a unique solution for measuring (n,2n) cross sections, which addresses all three of these concerns. This technique involves measuring a charged-particle reaction cross section, where the reaction populates the same compound nucleus as the reaction of interest.

As an example, directly measuring ^{241}Pu(n,2n) would require creating a thick target of the isotope, which has a 14.3 year half-life. With the surrogate approach, a thin target of ^{242}Pu could be used, which has the much longer half-life of 375,000 years. A convenient reaction for this example is (α,α') with a 55 MeV α-particle beam, and with this reaction, scattered beam should not produce a substantial neutron background. Fission will still create a neutron background, but the thin target allows for direct detection of many fission events, and the background can therefore be subtracted. A ratio would be taken between the surrogate reactions ^{241}Pu(α,α'2n) and ^{241}Pu(α,α'f), and by multiplying by the known ^{241}Pu(n,f) cross section, the ^{241}Pu(n,2n) cross section can to be deduced.

To perform these surrogate (n,2n) cross section measurements, a silicon telescope array has been placed along a beam line at the Texas A&M University Cyclotron Institute, which is surrounded by a large tank of Gadolinium-doped liquid scintillator, which acts as a neutron detector. The combination of the charge-particle and neutron-detector arrays is referred to as NeutronSTARS. In the analysis procedure for calculating the (n,2n) cross section, the neutron detection efficiency and time structure plays an important role. Due to the lack of availability of isotropic, mono-energetic neutron sources, modeling is an important component in establishing this efficiency and time structure.

This report describes the NeutronSTARS array, which was designed and commissioned during this project. It also describes the surrogate reaction technique, specifically referencing a ^{235}U(n,2n) commissioning measurement that was fielded during the past year. During the analysis of this measurement, it was found that the ^{235}U(n,f) neutron multiplicity could be extracted using a similar surrogate technique. A number detector challenges were encountered during this commissioning measurement, and improvements to the detector are planned for the next few months, before fielding the final

^{241}Pu(n,2n) and ^{239}Pu(n,2n) cross section measurements. Advanced multiplicity analysis techniques have been developed for this work, which should allow for efficient analysis of the two plutonium cross sections, once data has been acquired. Although experimental problems were found during analysis of the ^{235}U(n,2n) cross section, the ^{235}U analysis will continue while preparing for the plutonium cross section measurements, in order to extract as much useful detector and physics information as possible.

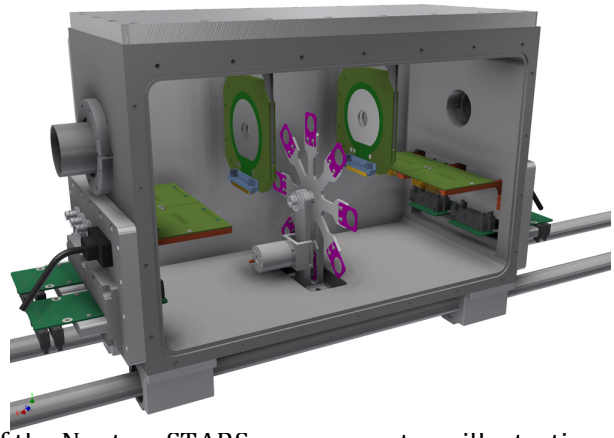

Fig. 1. A model of the NeutronSTARS vacuum system, illustrating vacuum components, electrical components, the target wheel, and the silicon detectors.

NeutronSTARS Detector System

The NeutronSTARS detector system includes a silicon telescope array for detecting light ions, as well as an additional silicon detector for measuring fission. These detectors are housed in an aluminum vacuum chamber, and a target wheel is positioned between the two sets of detectors. The design of the vacuum system can be seen in Fig. 1, with the silicon detectors separated for visibility.

The silicon telescope is positioned downstream of the target with regard to the beam direction. When an (α,α') event occurs in the target, energy is transferred to the target nucleus, and an α-particle of lower energy leaves the target. By correcting for two-body kinematics, the excitation energy of the residual nucleus can be calculated. In the

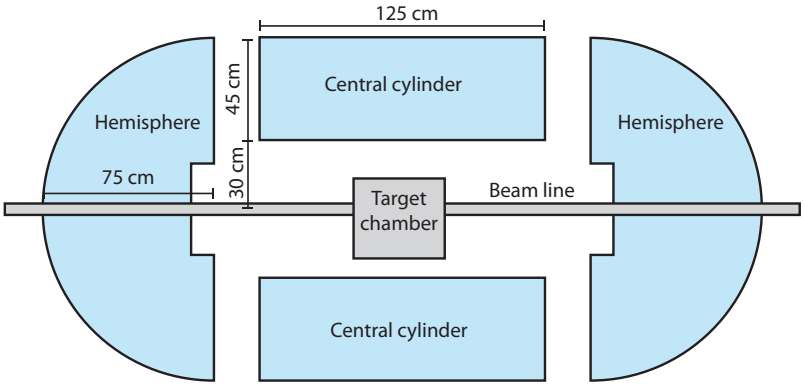

Fig. 2. A diagram of the Texas A&M Neutron Ball with the target chamber shown in the center.

angle range of 23° to 53° the particle is detected by the silicon telescope, with some amount of energy deposited in a 150 μm silicon detector, and the remainder deposited in a 1000 μm silicon detector. The relative energy deposited in the two detectors depends on the stopping power and total energy, and can be used to identify the type of particle. α-particles are the primary particle of interest, and other detected particles include protons, deuterons, tritons, and ^{3}He. A thin layer of aluminum foil protects the silicon detectors to prevent electrons, α-particles, and fission fragments from creating a large background in the telescope.

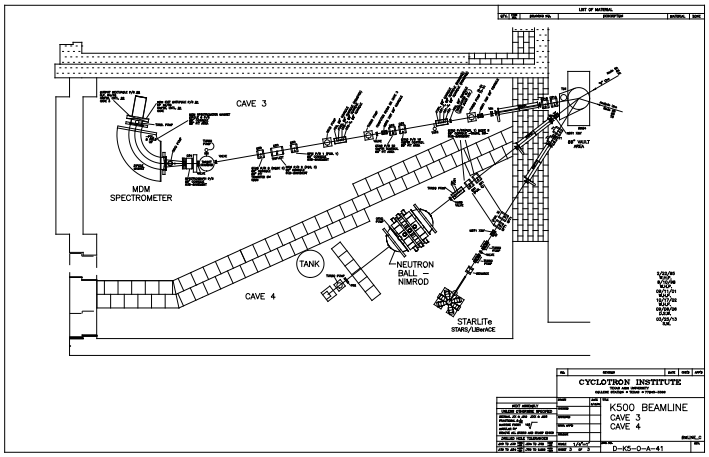

Fig. 3. Layout of Cave 4 at the Texas A&M Cyclotron Institute.

Upstream from the target is a 150 μm silicon detector, for detecting fission fragments. The detector is positioned close to the target in order to cover as large of an angle range as possible. As each fission event produces two fission fragments, the array efficiency for detecting a fission event is twice the efficiency for detecting a single fission fragment. There is little energy dependence for the detection efficiency of the fission detector, and the energy and efficiency can be calibrated in a straightforward manner using a ^{252}Cf source. The fission array efficiency is estimated to be about 35%.

The Texas A&M University Neutron Ball is utilized as the neutron detection portion of NeutronSTARS, and has been used previously in experiments with the NIMROD charged-particle array [2]. The array consists of six regions of 0.2% Gadolinium-doped pseudocumene liquid scintillator, and the liquid scintillator has a total weight of about 3.5 tons. Fig. 2 illustrates the dimensions of Neutron Ball, and shows the relative position of the target chamber, which contains the silicon array. The central cylinder shown is divided into four wedges, and the wedges are separated by about 10 cm. This leaves gaps in the array, which allow neutrons to escape, but this only decreases the detection efficiency by about 10%.

When a neutron enters Neutron Ball, it scatters off of the hydrogen in the liquid scintillator and quickly thermalizes. The cross section for ^{nat}Gd(n,γ) is very large at thermal energies, and the neutron quickly captures, producing a cascade of gamma rays. Liquid scintillator has a relatively long attenuation length for gamma rays, and the detector volume must be large in order to detect them. The gamma-ray interactions in the liquid

scintillator transfers energy to electrons, which interact with the liquid to produce scintillation light. The array efficiency for detecting neutrons does not have a straightforward estimate, as it can depend on the threshold energy cut, and neutron transport behavior. A Monte Carlo model can be used to identify the efficiency trend, and measurements can then be used to constrain the efficiency at specific energies.

Monte Carlo Modeling

During the design phase of NeutronSTARS, the software package Geant4 [3] was used for the Monte Carlo physics modeling of neutron interactions in the neutron detector. An existing simulation framework called GSim had been previously written by the author to provide a reliable simulation design format for Geant4, as well as providing time-dependent output diagnostics for the visualization program GView.

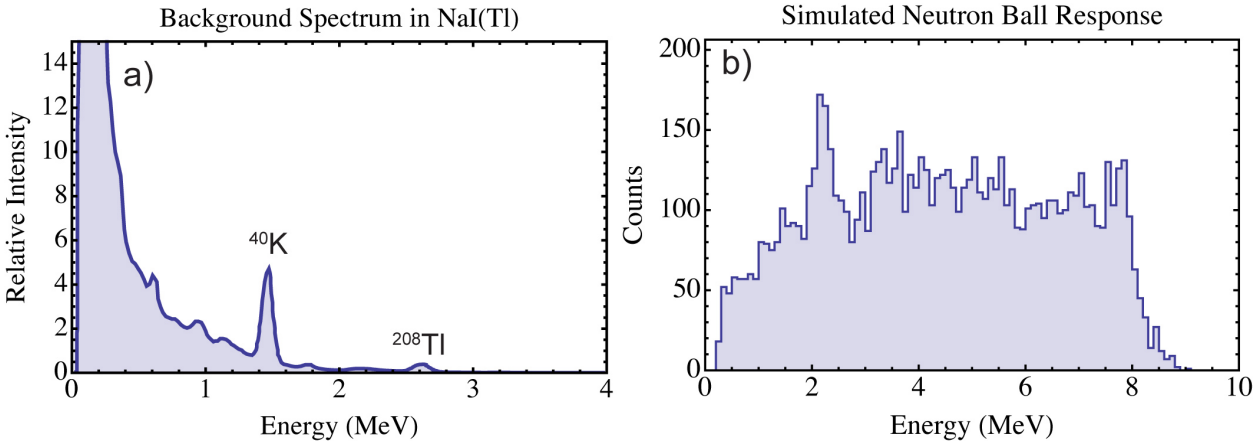

Fig. 4. a) Typical background spectrum in NaI(Tl) adapted from [4]. b) Detector response for 1 MeV neutrons simulated in Geant4.

The NeutronSTARS (n,2n) measurements are fielded in Cave 4 of the Texas A&M Cyclotron Institute. Fig. 3 shows the approximate layout of Cave 3 and Cave 4, which share a dividing wall, and Neutron Ball is shown on the right-hand side of the figure. The beam dump for the Neutron Ball beam line is not shown, and it consists of a large block of concrete attached to the lower wall.

The detector arrays shown in Figs. 1 and 2 were modeled in a Geant4 simulation, and the geometry of the concrete shown in Fig. 3 was also added to the model. The Geant4 simulation used the QGSP_BERT_HP physics factory, with the Livermore electromagnetism physics class overriding the default electromagnetism class contained in the factory. An isotropic source of neutrons was produced at the target position, and the absorbed gamma energy distribution as a function of neutron energy was calculated.

Although the Neutron Ball geometry is large enough to produce a signal for most neutrons, not all of the gamma ray energy from ^{nat}Gd(n,γ) is absorbed by the detector. This is due to the long attenuation length of gamma rays in the liquid scintillator. If all measured energies are assumed to originate from neutrons, the neutron detection efficiency can be as high as 80% for 1 MeV neutrons. However, the liquid scintillator is responsive to background gamma rays, which could be misinterpreted as neutrons, and an

energy threshold is needed to prevent this. Fig. 4a shows a typical NaI(Tl) detector background spectrum, illustrating the substantial background at low-energies, where the data shown is adapted from [4]. The 1.46 MeV gamma ray is from ^{40}K decay, and 2.61 MeV gamma ray is from ^{208}Tl decay, which is part of the ^{232}Th decay chain. Fig. 4b shows the Geant4 simulated detector response for 10,000 neutrons with 1 MeV of energy.

To eliminate backgrounds from ^{208}Tl decay, which originates from the ^{232}Th decay chain, an energy threshold can be placed on the measured detector energy. A cut of 2.8 MeV removes most backgrounds, but will reduce the neutron detection efficiency by about 20%. A balance must be found to optimize detection efficiency, while reducing background events, and this balance can be found experimentally. The energy spectrum shown in Fig. 4b can be directly measured with a ^{252}Cf source at the target position, and the Neutron Ball background can be measured by recording data with no sources.

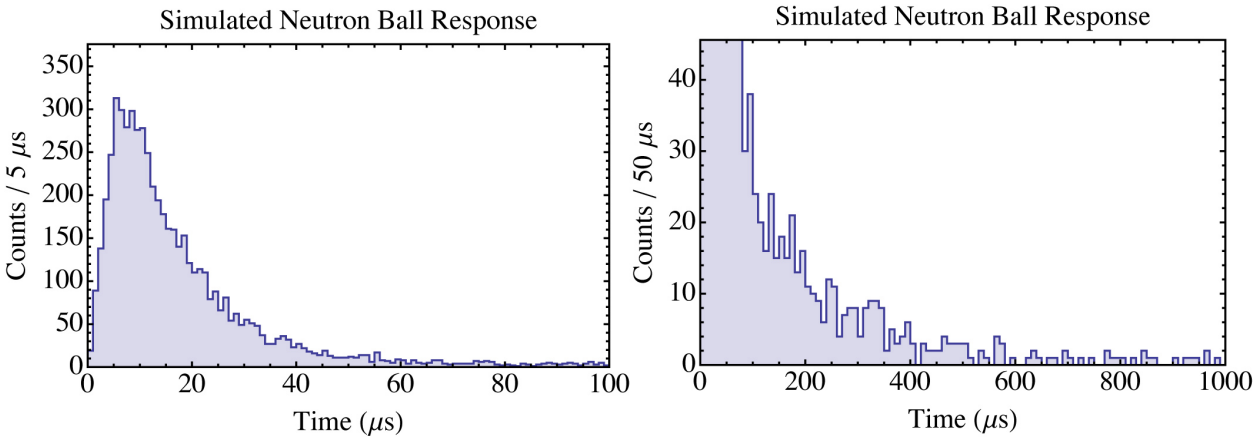

Fig. 5. Time response of Neutron Ball for 10,000 neutrons with 1 MeV of energy, calculated with Geant4. The energy threshold was set to 2.8 MeV.

As the neutrons thermalize before capturing on Gd, there is a time delay between the (α, α'2n) event and the detection of the neutron. This distribution can be calculated in Geant4, and the time spectrum for 1 MeV neutrons is shown in Fig. 5. There is a fast time component not shown, which would include gamma rays produced by the (n,2n) event, as well as gamma rays produced by inelastic scattering of neutrons on the carbon in the liquid scintillator. This signal will not help in identifying the number of detected neutrons, and is ignored.

The long average thermalization time of the neutrons limits the event rate at which the experiment can be fielded, and this translates to lower beam current than those used in typical surrogate reaction experiments. Many of the late-time neutrons thermalize in the liquid scintillator, and escape back into the target chamber volume. At low neutron energy, the flight across the central cavity can require hundreds of microseconds, which extends the time in which the system is busy.

Surrogate Ratio Method

The surrogate ratio method is a useful technique for determining neutron-induced reaction cross sections on short-lived targets, which would otherwise be unmeasurable.

This method was originally used by Cramer and Britt in 1970 [5,6], and has recently been used in the determination of several neutron-induced fission cross sections. The method begins with the assumption that compound nuclear decay is independent of compound nuclear formation. In a surrogate experiment, the compound nucleus of interest is produced using a direct reaction with a more accessible beam-target combination, and the decay of the compound nucleus is measured in coincidence with the outgoing particle from the direct reaction.

For fission applications, the Weisskopf-Ewing approximation is used, which ignores the difference in the angular momentum distribution between the neutron-induced and direct reactions. This approximation eliminates the need for theoretical descriptions of the direct reaction and compound decay. When employing the general surrogate reaction method, the total direct reaction cross section and the cross section including compound nuclear decay must be measured. The total cross section can be difficult to determine, as backgrounds from other reactions on contaminants can contribute to the total cross section. In addition, a full understanding of detector efficiencies is required.

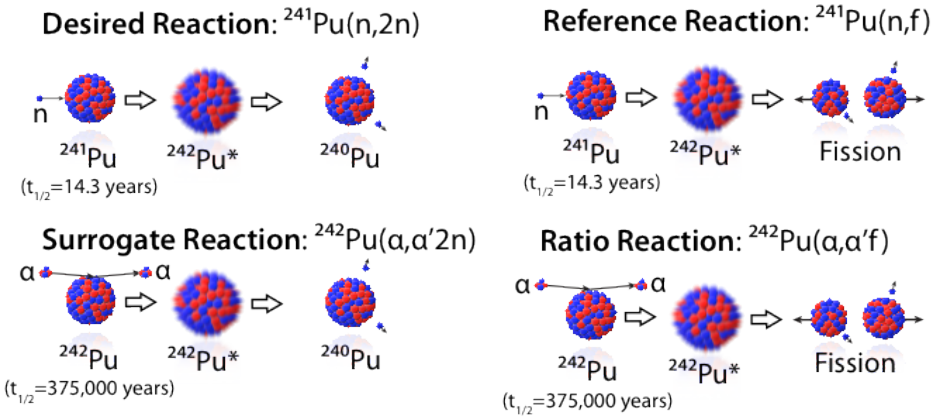

Fig. 5. A diagram of the surrogate ratio for ^{241}Pu(n,2n).

The surrogate ratio method is a variant of the more general surrogate method, which has a number of experimental advantages. In the case of a fission cross-section measurement, fission cross sections on two different targets are measured, and the ratio is multiplied by a known neutron-induced fission cross section. The benefit of this is that contaminants don't contribute to the channel of interest, and some of the detector efficiencies cancel in ratio. A past measurement performed by the surrogate reaction program measured the ^{240}Am(n,f) cross section using the ^{235}U(n,f) cross section as a reference:

$$\sigma\left(^{240}\mathrm{Am}(n,f),\mathrm{E}\right)=\frac{N\left(^{243}\mathrm{Am}(p,tf),\mathrm{E}\right)}{N\left(^{238}\mathrm{U}(p,tf),\mathrm{E}\right)}\times\frac{\sigma\left(^{240}\mathrm{Am}(n,\mathrm{CN}),\mathrm{E}\right)}{\sigma\left(^{235}\mathrm{U}(n,\mathrm{CN}),E\right)}\times\sigma\left(^{235}\mathrm{U}(n,f),\mathrm{E}\right)$$

where CN refers to the compound nuclear formation cross section, which is calculated theoretically for the two isotopes. For this work, (n,2n) reaction cross sections are the desired quantity, and a ratio will be used to known (n,f) reaction cross sections for the same nuclei. This has the benefit of eliminating the need for the compound nuclear formation cross section, as the two components of the ratio involve the same nucleus.

One specific reaction of interest for this work is ^{241}Pu(n,2n), and the surrogate inputs for this include the known ^{241}Pu(n,f) reaction cross section, as well as the ^{242}Pu(α,α'2n) and ^{242}Pu(α,α'f) reactions, which must be measured with the NeutronSTARS array. The surrogate ratio for this reaction is the following:

$$\sigma\left(^{241}\mathrm{Pu}(n,2n),\mathrm{E}\right)=\frac{N\left(^{242}\mathrm{Pu}(\alpha,\alpha'2n),\mathrm{E}\right)}{N\left(^{242}\mathrm{Pu}(\alpha,\alpha'f),\mathrm{E}\right)}\times\sigma\left(^{241}\mathrm{Pu}(n,f),\mathrm{E}\right)$$

The surrogate ratio method has been demonstrated for fission reaction cross sections for a large number of actinide targets, but has not previously been used to measure (n,2n) cross sections with detected neutrons. As such, the commissioning run for NeutronSTARS was chosen to confirm the known (n,2n) cross section ^{235}U(n,2n), which can be used to determine how accurate the technique will be, and identify any problems with the experimental conditions or analysis techniques.

Data Acquisition

A new data acquisition system was developed for the NeutronSTARS detector system. In the past, surrogate experiments used shaping amplifiers to convert charge-integrated signals into a form which could be recorded by peak-sensing ADCs. A separate branch of electronics would differentiate the signal and record the time that the signal occurred. This type of system is typically referred to as analog electronics. One common element in such a system is a trigger that directs the electronics to record the signal, which is followed by a veto that prevents the system from triggering again during a specified time. The trigger is typically open for 2-4 μs, which is incompatible with the neutron detection portion of this experiment, as the neutrons arrive over the course of 100 μs.

New Struck digitizers were programmed to allow for independent detection of each photomultiplier tube (PMT) signal. The digitizers have 14-bit resolution, and record traces at a frequency of 250 MHz. For high-resolution applications, filtering can allow for effective resolutions higher than 14-bits, but for scintillation signals, this is not necessary. The Struck digitizers record PMT signals separately from the triggered silicon events, and the data streams are later merged.

The ^{235}U(n,2n) Commissioning Experiment

The NeutronSTARS commissioning experiment was fielded in December 2015, and analysis of the experiment has been ongoing since that time. A 200 μg/cm^2 ^{236}U target was deposited on a 100 μg/cm^2 target backing, as the surrogate reaction for ^{235}U(n,2n) was chosen to be ^{236}U(α,α'2n). A number of other targets were irradiated as well, to identify sources of background and contamination in the data, including a blank target, a carbon target, and a lead target. The beam was chosen to have 25 ppA of current, which is significantly lower than the typical 1 pnA that is used during surrogate measurements. The lower current was chosen to reduce neutron backgrounds overlapping with the data, as neutrons are detected up to 100 μs after the event that produces them.

The 55 MeV α-beam was produced by the K150 cyclotron at the Texas A&M University Cyclotron Institute, and the experiment ran for seven days. The silicon telescope was calibrated with a ^{226}Ra α-source, and the fission detector was calibrated with a ^{252}Cf fission source. The same source was used to calibrate the neutron detector, as the neutron multiplicity distribution accompanying fission is known [7].

A number of problems were observed during the commissioning experiment, and have been studied over the course of the analysis. The most significant problem that occurred was that the scintillation energy spectrum did not reflect the expected distribution shown in Fig. 2b. After an in-depth literature search and a detailed analysis, it was concluded that Gd-loaded liquid scintillator had aged, and become opaque to the scintillation light. This type of scintillator has been used in a number of neutrino experiments in the past, and it was eventually discovered that the attenuation length of pseudocumene scintillation light can drop by 10% per year [8], where a 3 meter attenuation length was initially expected. The TAMU Neutron Ball is over 20 years old, and although it has been used for multiplicity measurements during the last decade, it appears as though the attenuation length has dropped to 30 cm.

The shorter attenuation length results in a substantial position sensitivity, as the detector was designed to allow light to be scattered throughout the chamber, and eventually be absorbed by the PMT. In its current state, only gamma rays that deposit energy near the PMT have a significant amount of light collection. Gamma rays in other areas of the detector can be detected, but have a significantly reduced energy. $^{12}C(\alpha,\alpha')$ reactions produce 4.4 MeV gamma rays, which allows for straightforward coincidence analysis. If the detector was functioning properly, one would expect a peak in the energy spectrum, representing the gamma ray energy. Fig. 6 shows the signal that was detected during the experiment on a log scale, illustrating that an exponential shape was observed in the energy spectrum. This indicates significant position sensitivity and attenuation.

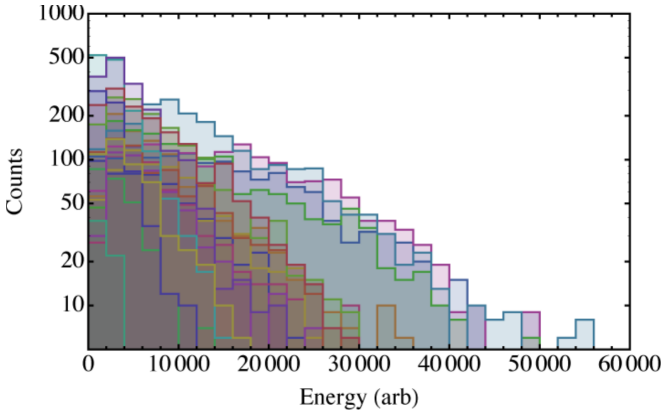

Fig. 6. Gamma ray spectrum detected by PMTs on log scale with 4.4 MeV $^{12}C(\alpha,\alpha')$ gamma ray.

As was shown in Fig. 4a, cutting background gamma rays from the data is an important part of maintaining a low-background for neutron multiplicity measurements. With the light attenuation that occurred during the experiment, it is not possible to separate neutrons from background gamma rays, and an energy cut cannot be used. This does not preclude analysis of the data, but simply causes a larger neutron background to be observed. The aged liquid scintillator is scheduled to be replaced before fielding the $^{239}Pu(n,2n)$ and $^{241}Pu(n,2n)$ experiments.

Another problem that was observed during the experiment was PMT after pulsing. Fig. 7 shows the time difference spectrum observed for ^{252}Cf decay data, with a clearly defined signal contribution and background contribution. The signal contribution results from neutrons thermalizing in the liquid scintillator over the time scale of tens of

microseconds, and then capturing on gadolinium. The gamma-cascade from the neutron capture is detected by the liquid scintillator, and the recorded time is tallied in the time difference distribution. The displayed events are calibrated to have time 0 correspond to the time of fission fragment detection.

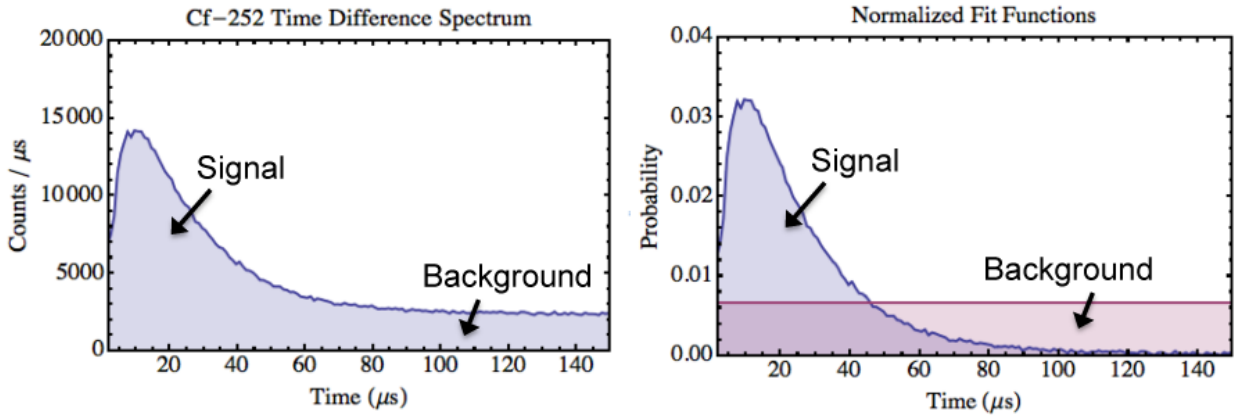

Fig. 7. Time difference spectrum for fission neutron detection from ^{252}Cf spontaneous fission. Fit functions derived from this distribution are shown on the right.

The background distribution corresponds to gamma rays and neutrons that are detected with random timing, implying that they are uncorrelated with the fission event that triggered the system. If the system were triggered randomly, rather than triggering on a fission fragment, a flat distribution would be expected. The PMT noise that was observed during the experiment manifested as a step in the time distribution, and an example of this is shown in Fig. 8. This noise is a problem in the interpretation of the data, as it occurs at the same time as signal neutrons. To correct this for the ^{235}U(n,2n) commissioning experiment, these channels were turned off, resulting in a lower neutron detection efficiency. The PMTs used in the experiment were old, and ion-afterpulsing is suspected of causing the noise. These PMTs are scheduled to be replaced before the ^{239}Pu(n,2n) and ^{241}Pu(n,2n) measurements.

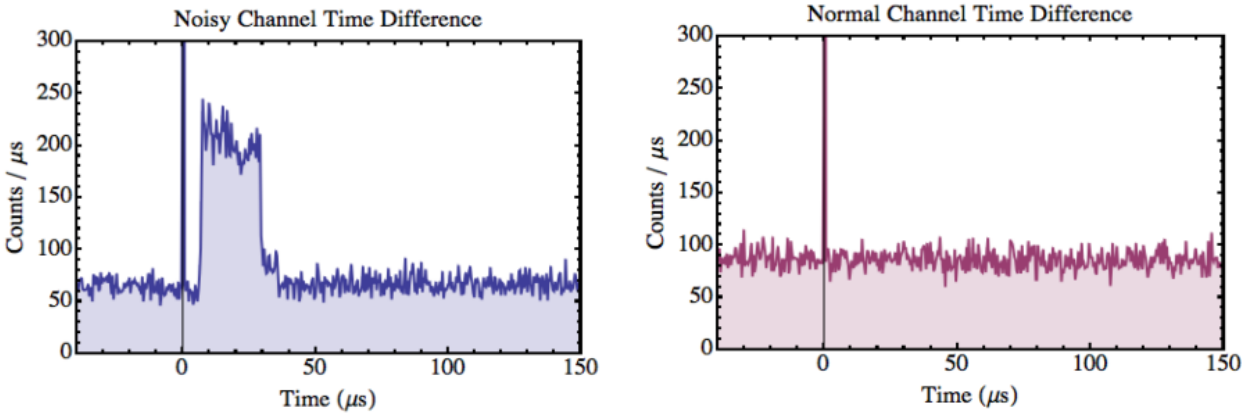

Fig. 8. A time difference spectrum for a noisy channel and a normal channel.

After correcting for kinematic shifts, the raw alpha distribution and fission coincident alpha distributions can be measured. Fig. 9 shows both of these distributions, and the large peak at zero excitation energy of the raw spectrum is the ^{236}U(α,α') elastic peak. The fission excitation energy spectrum is negligible below the fission barrier, and becomes large at an energy slightly below the neutron separation energy. This indicates that ^{235}U(n,f) has a large cross section for low neutron energies. The statistics drop at high energy is due to the alpha-particle Coulomb barrier. The excitation energy represents the difference between the incoming and outgoing alpha particle energy, and above 35 MeV excitation energy, the alpha does not have enough energy to escape the nucleus.

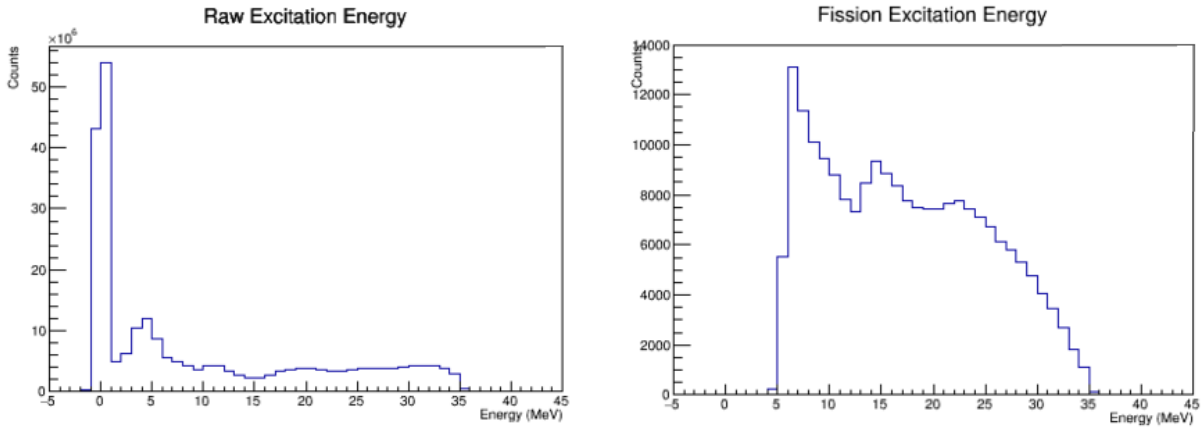

Fig. 9. Raw alpha excitation spectrum and fission-coincident excitation spectrum.

The large difference in statistics between the raw alpha and fission-coincident spectra at high excitation energy was unexpected, as it indicates that the alpha particle is scattering off of a significant amount of non-^{236}U material. The 100 μg/cm^2 carbon backing on the target can account for some of this, but additional material is suspected. Examining the fission fragment energy distribution can give a sense of fission fragment energy loss in the target, and help in identifying the anomalous target material. Fig. 10 shows the fission fragment energy spectra for the ^{252}Cf source and ^{236}U target. The ^{252}Cf demonstrates the expected fission fragment profile, with both light and heavy fragment distributions visible. The ^{236}U target on the other hand looks highly degraded, indicating that there is a significant amount of energy loss in the target. This additional energy loss will be investigated before the ^{239}Pu(n,2n) and ^{241}Pu(n,2n) experiments are fielded.

The neutron time-difference spectrum for ^{236}U data can be plotted in a similar way as the ^{252}Cf data shown in Fig. 7, and this can be seen in Fig. 11. The fission neutron time-difference plot has a very similar structure as the ^{252}Cf fission data, indicating that the in-beam fission data can be analyzed in the same way as the ^{252}Cf fission calibration. The raw neutron time-difference plot has a much larger background, corresponding to the excess (α,α') events in the raw excitation energy spectrum shown in Fig. 9. The main consequence of this additional background is a lower signal/noise ratio, resulting in larger uncertainties. Reducing this background would require a reduced number of (α,α') events on non-^{236}U material in the target.

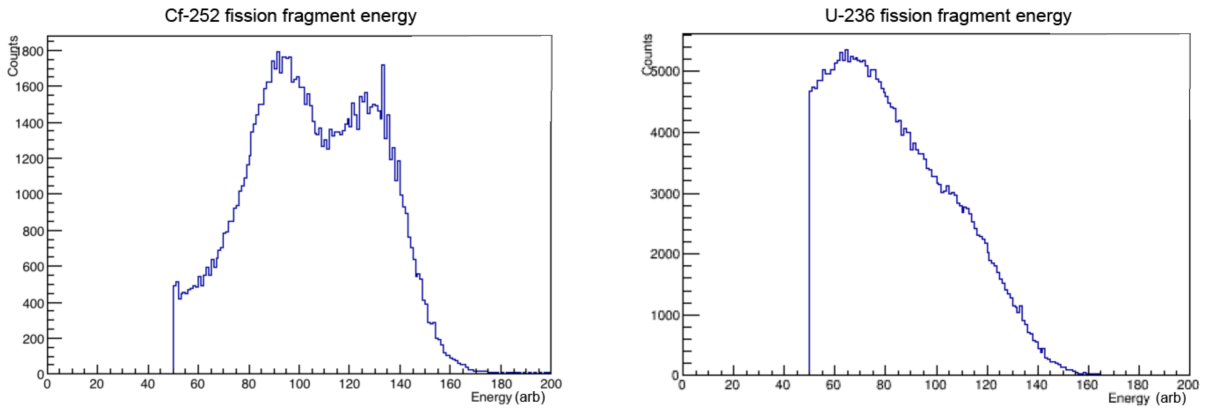

Fig. 10. Fission fragment energy spectra from the ^{252}Cf source and ^{236}U target. The cut at channel 50 is meant to remove alphas from carbon break-up in the fission signal.

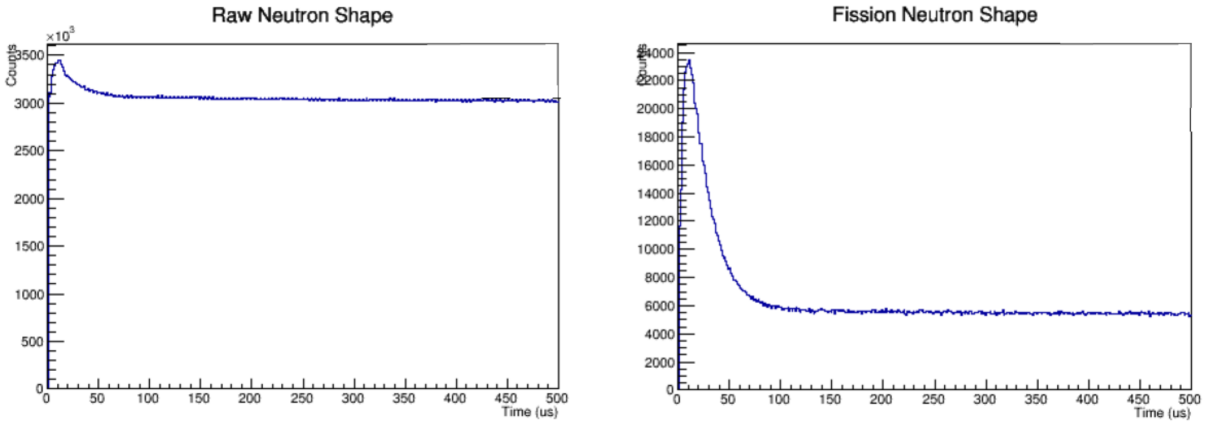

Fig. 11. Neutron time difference distributions for the ^{236}U(α,α') data. The raw neutron shape plot shows events without fission coincidence. The fission neutron shape plot includes fission coincidence.

Multiplicity Analysis of ^{252}Cf

Measuring (n,2n) cross sections on actinides requires statistical analysis of the neutron multiplicity distributions. The first important concept in the multiplicity analysis is recognizing that the detector is not 100% efficient, which means that the number of detected neutrons does not directly correspond to the number generated neutrons in the event. In addition to this, a number of background particles can be detected in the same time window as signal neutrons, resulting in a distortion of the neutron multiplicity distribution. Fig. 12 shows the convolution of the ^{252}Cf multiplicity distribution with a binomial distribution, to produce the convolved detected neutron distribution expected during an experiment.

To establish the validity of the analysis procedure, and to calibrate the detector array, the neutron multiplicity distribution for ^{252}Cf was analyzed. The time-difference spectrum was shown in Fig. 7, with a signal multiplicity per event integrated from 0 μs to 150 μs. A background multiplicity was defined by integrating from 350 μs to 500 μs, which occurs after the neutron time difference spectrum has returned to a flat background. Fig. 12 shows the integrated ^{252}Cf multiplicity distributions for the signal and background region. If the background was assumed to be entirely random, a Poission distribution would be expected. The data appears to have non-Poissonian behavior at high

multiplicities, which indicates correlated events, either from un-triggered fission events or cosmic ray spallation. The non-Poissionian behavior can be accounted for by including the background data in the multiplicity analysis, rather than the Poisson distribution.

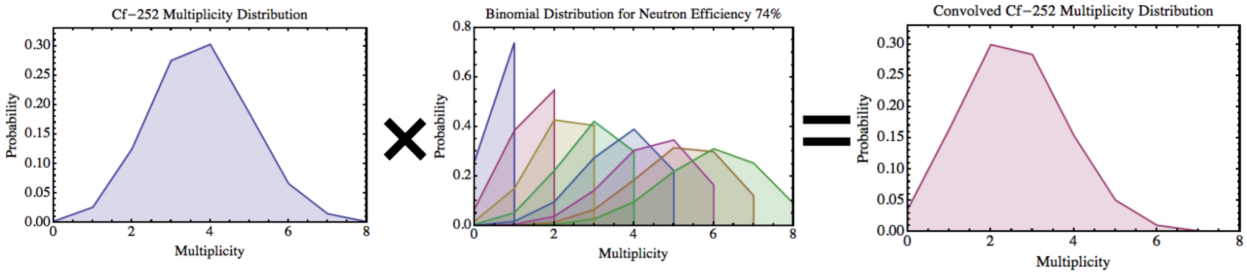

Fig. 12. (left) ^{252}Cf multiplicity distribution from literature [7] is convolved with a binomial distribution representing a neutron detection efficiency of 74%, producing the convolved distribution that would be expected in the data.

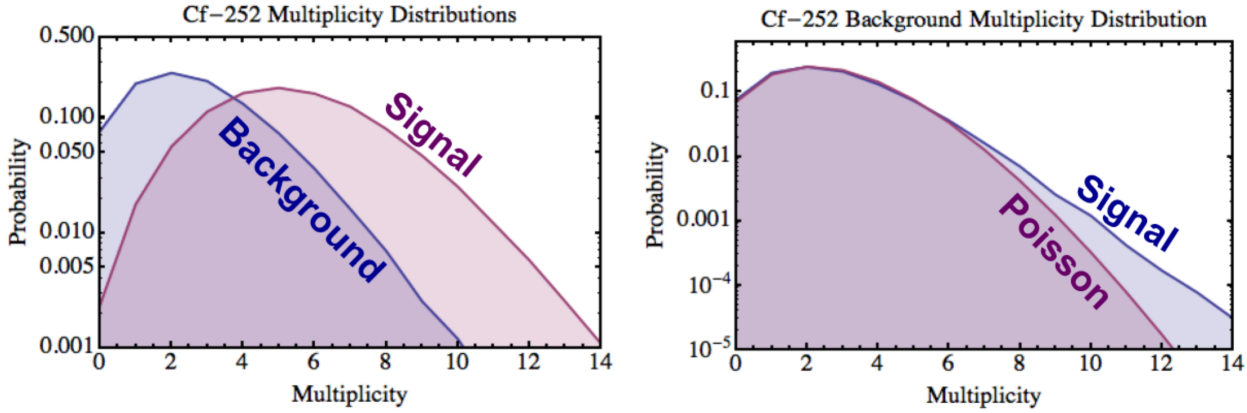

Fig. 13. (left) ^{252}Cf multiplicity distribution for the signal region and background region. (right) The background region is compared to a Poisson distribution, indicating that correlated events occur.

To solve for the ^{252}Cf fission neutron multiplicity, the signal neutron multiplicity must be deconvolved using the background neutron multiplicity. This can be done in the form of a linear equation, where the signal distribution is equal to a background matrix times the real number of neutrons detected. By inverting the background matrix, the number of detected neutrons can be solved for using the signal neutrons. Another approach involves using a linear regression to fit the signal distribution with shifted background distributions, where the fit coefficients correspond to the number of detected neutrons.

The method developed for this work is more sophisticated than these two approaches, and leverages the actual time difference shape of the signal and background neutrons, rather than by integrating the multiplicity distribution over two time windows. Fig. 14 shows an example of how to fit the 0 detected neutron and 1 detected neutron contributions using multiplicity 1 data. a_0 corresponds to events with 0 detected neutrons, and a_1 corresponds to events with 1 detected neutron. mb_0 and mb_1 refer to the background multiplicities for 0 and 1 neutrons respectively, which are shown in Fig. 13.

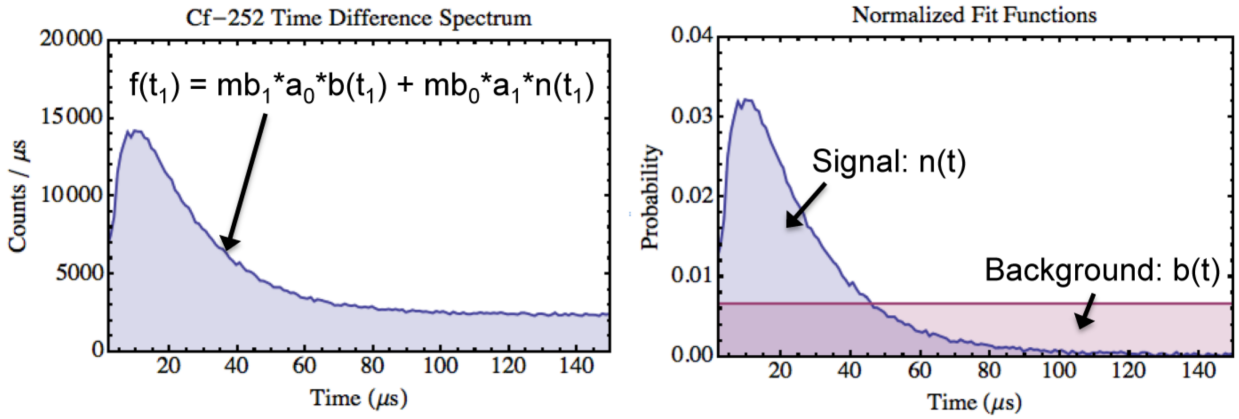

Fig. 14. (left) The multiplicity 1 data to be fit, where mb_N is the background multiplicity for N neutrons and a_N is the number of detected neutrons with multiplicity N. (right) The fit functions derived from the time-difference data itself.

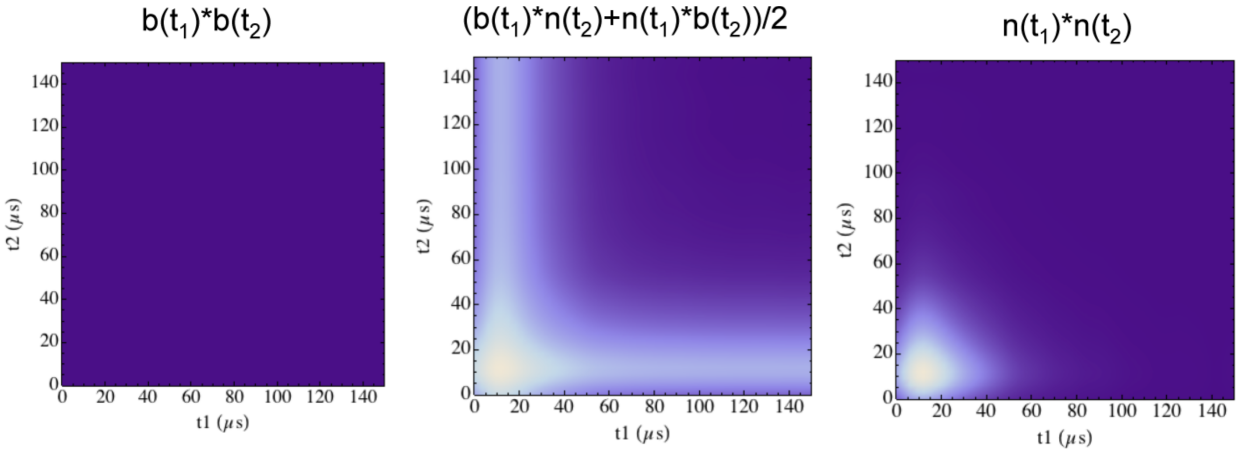

Fig. 15. The three two-dimensional fit functions used to fit multiplicity 2 data.

The multiplicity 1 data shown in Fig. 14 is a special case, and the method can be extended to higher dimensions. For multiplicity 2 data, there are 3 possible fit functions that are used to fit the data: 2 background, 1 neutron/1 background, and 2 neutrons. Fig. 15 illustrates what these fit functions look like for NeutronSTARS data, where the 1 neutron/1 background data has been symmetrized. From this data, the 0 neutron, 1 neutron, and 2 neutron statistics can be fit, whereas the multiplicity 1 data could only fit 0 neutron and 1 neutron statistics. Higher multiplicities can be fit to produce higher detected neutron multiplicities, but the statistics are constrained by the background data shown in Fig. 13. The various multiplicities are fit using the following series of fit functions:

- $f(t_1) = mb_1*a_0*b(t_1) + mb_0*a_1*n(t_1)$
- $f(t_1,t_2) = mb_2*a_0*b(t_1)*b(t_2) + mb_1*a_1*(n(t_1)*b(t_2)+b(t_1)*n(t_2))/2 + mb_0*a_2*n(t_1)*n(t_2)$
- $f(t_1,t_2,t_3) = mb_3*a_0*b(t_1)*b(t_2)*b(t_3) + mb_2*a_1*(n(t_1)*b(t_2)*b(t_3)+b(t_1)*n(t_2)*b(t_3)+b(t_1)*b(t_2)*n(t_3))/3 + mb_1*a_2*(n(t_1)*n(t_2)*b(t_3)+n(t_1)*b(t_2)*n(t_3)+b(t_1)*b(t_2)*n(t_3))/3 + mb_0*a_3*n(t_1)*n(t_2)*n(t_3)$
- …

where mb_N is the background multiplicity probability for N particles, and a_N in the number of detected neutrons.

The structure of these fit functions is related to binomial coefficients, and as can be seen in Fig.13, the data extends beyond multiplicity 10. The complexity of these fit functions expands exponentially with multiplicity, and would require an unreasonable amount of computing power to calculate the fit directly for higher multiplicities. During the analysis of the ^{252}Cf, an algorithm was developed to reduce the exponential complexity down to quadratic complexity, significantly reducing the computation time for high multiplicities. The procedure resembles the Pascal's triangle method for calculating binomial coefficients.

a)

	b	n
1	0.3	0.5
2	0.4	0.2
3	0.8	0.1
4	0.3	0.7

b)

Fit Function \ Detected Neutrons	0	1	2	3	4
0	1	0	0	0	0
1	0.3	0.5	0.	0.	0.
2	0.12	0.26	0.1	0.	0.
3	0.096	0.22	0.106	0.01	0.
4	0.0288	0.1332	0.1858	0.0772	0.007

Fig. 16. Example of the numerical procedure for constructing the high-multiplicity fit functions. a) Example values for $b(t_N)$ and $n(t_N)$. b) Matrix where fit function terms are calculated row-by-row, adding an additional neutron for each row.

In this procedure the $b(t_N)$ and $n(t_N)$ terms are evaluated, and a matrix is calculated row-by-row using the result of the lower multiplicity fit function to derive the higher multiplicity fit function. Fig. 16 illustrates this, where the fit function 1 row in Fig. 16b is the same as row 1 of Fig. 16a. For the next row, $b(t_2)$ and $n(t_2)$ are combined with the fit function 1 row to represent the impact of adding one extra particle on the probability sum. For each new row, a single neutron is added, resulting in quadratic computational complexity. To use the detected neutron fit function matrix in the actual fit functions, each term must be divided by the appropriate binomial coefficient.

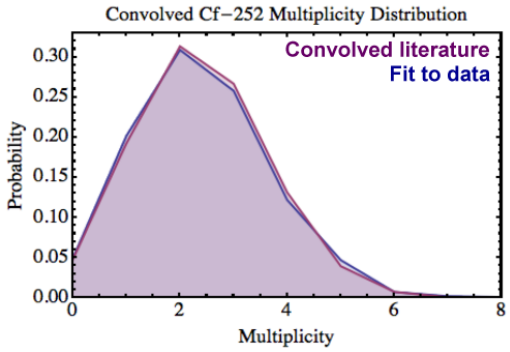

Fig. 17. Comparison of multiplicity fit to data with the literature ^{252}Cf multiplicity distribution convolved with the binomial distribution.

Combining the various multiplicity fits into a global neutron multiplicity fit allows for the determination of the ^{252}Cf multiplicity distribution. Fig. 17 shows a comparison of the neutron multiplicity fit to the literature ^{252}Cf multiplicity convolved with the neutron efficiency binomial distribution.

Multiplicity Analysis of ^{236}U(α,α')

The surrogate reaction for the commissioning ^{235}U(n,2n) experiment is ^{236}U(α,α'2n), where "2n" is one of many possible exit channels for the ^{236}U(α,α') reaction. The ^{235}U(n,2n) cross section can be calculated using the standard surrogate method by using the ratio of the ^{236}U(α,α'2n) reaction rate to the total ^{236}U(α,α') reaction rate, and by multiplying by the compound formation cross section. This method requires a precise understanding of target contaminants and efficiencies. The surrogate ratio method approach used in this work compares the ^{236}U(α,α'2n) reaction rate to the ^{236}U(α,α'f) reaction rate, which is then multiplied by the ^{235}U(n,f) cross section. The benefit of tagging on fission events is that target contaminants should not be significant in either the ^{236}U(α,α'2n) reaction or the ^{236}U(α,α'f), simplifying the analysis.

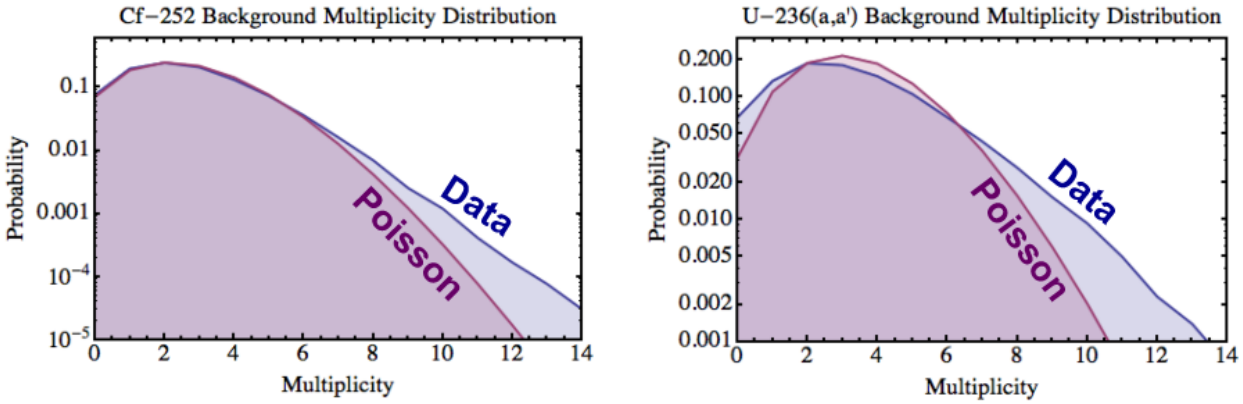

Fig. 17. Comparison of background multiplicity distributions for ^{252}Cf and ^{236}U(α,α').

The neutron multiplicity analysis for ^{236}U(α,α') can be performed in much the same way as ^{252}Cf, and one of the important ingredients in this analysis is the background multiplicity distribution. As was discussed previously, uncorrelated background events should follow a Poisson distribution. Fig. 17 shows the background multiplicity comparison to a Possion distribution for the ^{252}Cf and the ^{236}U(α,α') data. The ^{252}Cf spontaneous fission data differs from the Poisson distribution at high multiplicity, and this is expected to result from correlated neutrons in cosmic ray spallation. The ^{236}U(α,α') background multiplicity differs dramatically from Poisson at most multiplicities, and this is likely due to the large ^{236}U(α,f) fusion-fission cross section. This reaction is expected to have a large neutron multiplicity, and although the fission events should be randomly distributed through time, they will produce correlated bursts of neutrons. The non-Poissonian background is not a significant problem, as the data itself is used in the analysis.

As the ^{236}U(α,α'f) fission time difference spectrum in Fig. 11 has a similar shape as the ^{252}Cf fission time difference spectrum, shown in Fig. 14, it is expected that the multiplicity analysis will be similarly successful. The arbitrary-dimension neutron multiplicity fitting algorithm described in the previous section has currently only been tested on the ^{252}Cf calibration data, and will need to be configured to allow for multiplicity fitting of finite alpha energy ranges, specifically to match the energy bin structure of Fig. 9.

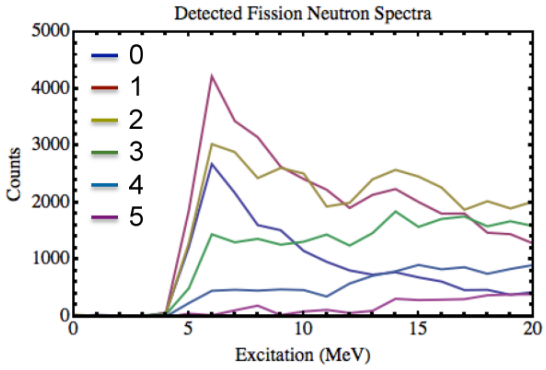

Fig. 17. Preliminary detected fission multiplicity data with 1 MeV bins for ^{236}U(α,α'f) data.

For preliminary tests, a narrow time cut was applied to the time difference spectrum to reduce backgrounds as much as possible, and a variant of the linear algebra approach was applied. Beginning from low multiplicities, higher neutron multiplicities were calculated sequentially. Fig. 17 shows the preliminary fission multiplicity distribution with 1 MeV bins for the ^{236}U(α,α'f) data. This data can be combined into larger energy bins and plotted on a neutron multiplicity axis, and this result is shown in Fig. 18 for MeV energy bins.

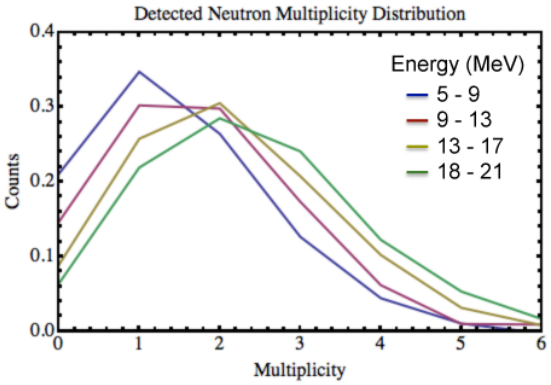

Fig. 18. Preliminary detected fission neutron multiplicity distribution for ^{236}U(α,α'f) data.

Neutron multiplicity distributions from fission are typically expected to have a Gaussian shape, but directly measuring the multiplicity distribution can be extremely challenging without a high-efficiency neutron detector. NeutronSTARS has a neutron detection efficiency on the order of ε=60%, and the efficiency for detecting a multiplicity N event is ε^N. For NeutronSTARS, the probability for detecting a multiplicity 6 event is 0.05. For a 1% efficient neutron detector array, which is more common, detecting such event would have a probability of 10^{-12}. This implies that such a detector would on average detect one event per trillion, and nuclear physics experiments typically do not have such large statistics.

Due to the difficulty of measuring high multiplicity events, fission multiplicity measurements typically only measure the mean of the neutron multiplicity distribution. This procedure includes the typical challenges associated with measuring neutron-producing reactions on actinides, and measuring the mean as a function of neutron energy

can be difficult. NeutronSTARS uses the surrogate method, which allows for measurements on short-lived isotopes, and also provides a measure of effective neutron energy by design.

The result shown in Fig. 8 is a benchmark of neutron multiplicity surrogate measurements for (n,f), and the result will be compared to literature values. A successful benchmark would confirm that NeutronSTARS can be used to measure (n,f) neutron multiplicity on short-lived actinides, and this could be an interesting physics result in itself. The future (n,2n) cross section measurements contain the relevant data for such analyses, and will be analyzed for (n,f) neutron multiplicity information, in addition to the (n,2n) cross section.

The neutron multiplicity result shown in Fig. 18 will be analyzed using the advanced fitting algorithms described in this report in order to reduce statistical uncertainties in the result. The detected neutron multiplicity is a convolution of the generated neutron multiplicity with the binomial distribution, and the data in Fig. 18 would need to be deconvolved in order to produce the generated neutron multiplicity distribution. This procedure tends to amplify noise in the data, and a fit with a Gaussian distribution may be a more appropriate way to establish the distribution.

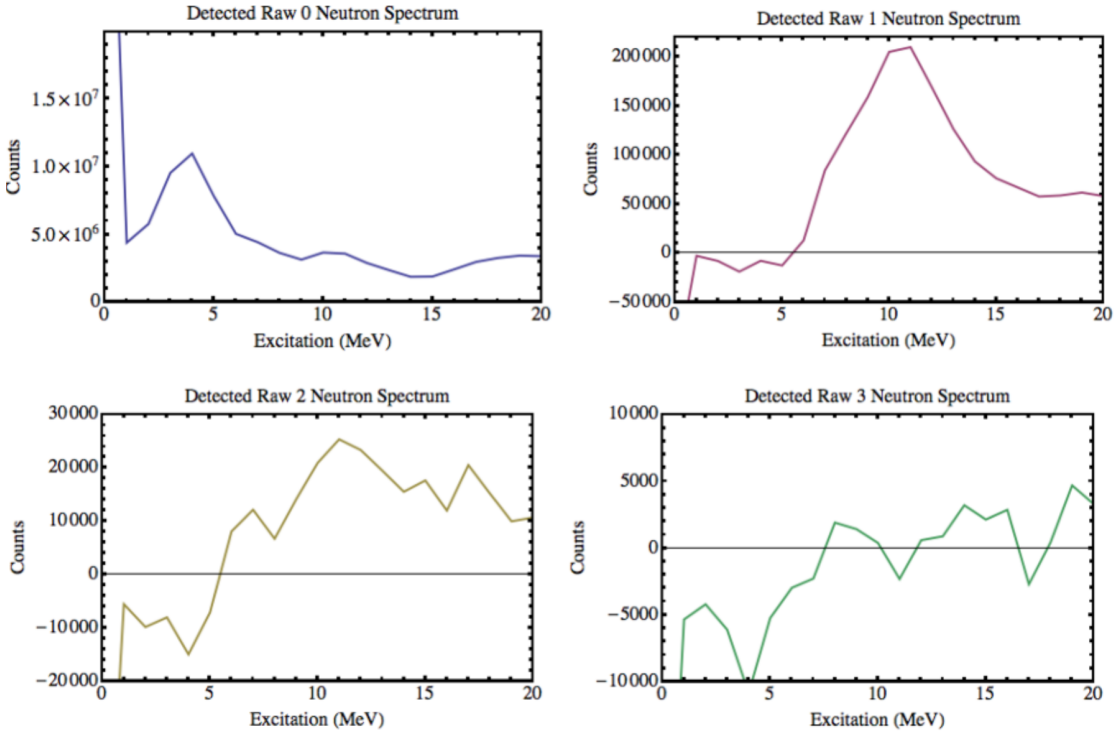

Fig. 19. Preliminary detected neutron spectra for a variety of multiplicities in the raw ^{236}U(α,α') data.

Two objectives of this project are to measure the ^{239}Pu(n,2n) and ^{241}Pu(n,2n) cross sections. The ^{235}U(n,2n) commissioning experiment was meant to identify any challenges in the experimental conditions and analysis, and a number of problems were found which may preclude producing an accurate ^{235}U(n,2n) cross section. The main problem is opaqueness of the aged liquid scintillator, and the after-pulsing of the old PMTs. These issues prevented energy information from being extracted from the data, which resulted in large neutron background rates. The large background rate combined with the

anomalously high inelastic alpha-scattering rate resulted in a large background in the raw neutron time-difference spectrum, which was intended to look more like the fission-coincident time-difference spectrum shown in Fig. 11 (right).

In the future, the structure of the background in Fig. 11 (left) will be analyzed more precisely by examining the alpha energy dependence of the time-difference spectra, in order to determine the shape of neutrons and backgrounds in the raw distribution. In addition, the multidimensional fitting algorithm will be applied to reduce uncertainties resulting from these backgrounds. A preliminary analysis of the fission-subtracted raw detected-neutron distributions has been performed, and the results are shown in Fig. 19.

Future Improvements

There is a straightforward path to solving many of the experimental problems that occurred during the commissioning experiment. The first and most important improvement is replacing the aged liquid scintillator. This improvement will allow for light transport in the detector, and should dramatically reduce position sensitivity. The energy resolution should be significantly improved, allowing for many backgrounds to be removed from the data. As was described in the previous sections, backgrounds are the limiting factor in extracting the (n,2n) cross section. Quotes have been obtained for replacement EJ-335 liquid scintillator from Eljen. The scintillator contains mineral oil, which is intended to stabilize the scintillator, and the Gd doping level is 0.25%.

Past modeling of NeutronSTARS used Geant4 to simulate the neutron, gamma, and electron interactions, but did not include optical transport through the liquid scintillator, or optical scattering off of the reflective paint on the inner surface of the neutron detector. Geant4 has the capability of modeling optical transport, including scintillation, attenuation, reflection, and absorption processes. While upgrades are being made to the NeutronSTARS array, Geant4 modeling will be used to simulate both the original array and the upgraded array. These simulations will help in interpreting the data from the commissioning experiment, and may reveal specifically which sources of background affected that experiment.

The other array upgrade underway is the replacement of all photomultiplier tubes. As was shown in Fig. 8, several of the existing PMTs have noise problems, potentially resulting from ion-afterpulsing. This background disrupts the neutron time-difference analysis, and these PMTs have been disabled in the present analysis, resulting in a lower neutron-detection efficiency. The new PMTs should not have this problem, and will allow for all PMTs to be included in the data analysis in the future. The replacement B133D01S PMTs have a 5” diameter, and are manufactured by ADIT Electron Tubes.

While the NeutronSTARS array upgrade is underway, analysis will continue on the ^{235}U(n,2n) commissioning experiment. The new arbitrary-dimension fitting algorithm will be applied to extract the neutron multiplicity spectrum from fission as accurately as possible, which may result in a peer-reviewed publication. The new algorithm will also be applied to the (n,2n) analysis, but it is not yet clear whether the detector problems from the commissioning experiment will allow for the extraction of a reliable ^{235}U(n,2n) cross section. The ^{239}Pu(n,2n) and ^{241}Pu(n,2n) experiments will be fielded once the array upgrades are complete. This work was funded by the Office of Defense Nuclear Nonproliferation Research and Development within the U.S. Department of Energy's National Nuclear Security Administration under contract DE-AC52-07NA27344.

References

[1] J. E. Escher *et al.*, RMP **84**, 353 (2012).
[2] R. P. Schmitt *et al.*, NIM A **354**, 487 (1995).
[3] S. Agostinelli *et al.*, NIM A **506**, 250 (2003).
[4] A. L. Mitchell, R. T. Kouzes, J. D. Borgardt, PNNL-18666, PNNL, 2009.
[5] J. D. Cramer and H. C. Britt, Nucl. Sci. Eng. **41**, 177 (1970).
[6] J. D. Cramer and H. C. Britt, Phys. Rev. C **2**, 2350 (1970).
[7] J. W. Boldeman and M. G. Hines, Nucl. Sci. Eng. **91**, 114-116 (1985).
[8] Brian M. Cook, Ph. D. Thesis, California Institute of Technology (1996).